Polarization Multiplexing and Demultiplexing for Appearance-Based Modeling

Oana G. Cula, *Member*, *IEEE*,
Kristin J. Dana, *Member*, *IEEE*,
Dinesh K. Pai, *Member*, *IEEE*, and
Dongsheng Wang

Abstract—Polarization has been used in numerous prior studies for separating diffuse and specular reflectance components, but in this work we show that it also can be used to separate surface reflectance contributions from individual light sources. Our approach is called *polarization multiplexing* and it has a significant impact in appearance modeling where the image as a function of illumination direction is needed. Multiple unknown light sources can illuminate the scene simultaneously, and the individual contributions to the overall surface reflectance are estimated. Polarization multiplexing relies on the relationship between the light source direction and the intensity modulation. Inverting this transformation enables the individual intensity contributions to be estimated. In addition to polarization multiplexing, we show that phase histograms from the intensity modulations can be used to estimate scene properties including the number of light sources.

Index Terms—Reflectance, surface reflectance, specular reflectance, body reflectance, diffuse reflectance, polarization, multiplexing, appearance, appearance-based modeling.

1 Introduction

Polarization of reflected light provides a wealth of information not available in scalar intensity images. It is well known that polarization of light is a useful quantity for separating surface reflectance from body reflectance because surface reflectance maintains the polarization of the source, while body reflectance becomes depolarized. Appearance-based modeling requires images from multiple illumination and viewing directions, so bidirectional imaging is a common tool for capturing appearance [1], [8], [23], [12], [11], [17], [4], [2]. In certain modeling tasks, it is important to separate the body and surface reflectance components to determine how each varies with illumination and view. For example, these two components may be interpolated differently for the appearance-based representation. The surface component contains roughness that changes appearance abruptly with illumination and view (high frequency variations), while the subsurface component is more diffuse (low frequency variations). Therefore, the surface component requires a denser sampling of the illumination/view space. One area where layered representations have become particularly useful is in modeling the appearance of human skin [7], [16], [4], [10], [5].

The particular use of polarization in image-based modeling has received sparse attention in the literature. Our goal is to employ polarization not only for separating surface and subsurface reflectance, but also for estimating reflectance from individual light source directions. If individual ordinary light sources are used in isolation, longer exposure times are needed to avoid dim images. Longer exposure times are not acceptable when imaging moving objects. For example, even the slight motions due to breathing will blur details in high-resolution human face images. We develop a novel method called *polarization multiplexing* to isolate the contribution of surface reflectance from the individual unknown light sources.

Polarization of reflected light has been used in numerous ways by vision researchers. The polarization angle of reflected light has been used as a cue for image segmentation [26], [25], for shape estimation [18], [19], [20], [13] and for separating diffuse and specular reflectance components [15], [4], [22]. However, the use of polarization for multiplexing light source directions is novel.

It is well known that when linear polarizers are used on the light source and camera, the image intensity is modulated by a sinusoid. Further analysis reveals that when the plane of the polarizer is not restricted to be perpendicular to the illuminating ray, the modulating sinusoid also depends on the light source direction. We show that this modulation can be used to estimate the contribution from each light source even when all light sources are *unknown* and illuminate the scene *simultaneously*. Note that polarization multiplexing has a similar goal to illumination multiplexing [21], namely, to determine the contribution from a single illumination direction. However, polarization multiplexing does not use an off/on spatial pattern of light sources but instead uses a rotating polarizer at the camera to get a pattern of modulation coefficients.

Because the phase of the intensity modulation depends on the light source direction, we can use phase clustering to reveal the number of light sources in the scene. Another method that estimates the light source distribution using polarization is described in [14], but the method is fundamentally different because it detects intensity maxima in the image to find specularities. For our approach, phase histograms are constructed and clusters reveal the light source number, as well as the extent of the light source.

2 Polarization Multiplexing Method

We assume that for a given camera direction, the scene is viewed with multiple light sources. These light sources are behind a linearly polarized sheet called the source polarizer as shown in Fig 1. A second linear polarizer called the camera polarizer is placed on the camera. The polarizer at the light source is fixed and the polarizer at the camera can rotate. Assume there are N light sources given by s_j, $j \in [1..N]$. For a fixed camera position, we assume the viewing direction v is approximately constant over the image.

The surface reflectance from a point due to a set of light sources is modulated by a sinusoid that is a function of the camera polarizer angle and the light source directions, as illustrated in Fig. 2. As an example, consider three light sources simultaneously illuminating the scene. Let $[I(\theta_{c1})\ I(\theta_{c2})\ I(\theta_{c3})]$ be the measured images with three different rotation angles of the camera polarizer $[\theta_{c1}\ \theta_{c2}\ \theta_{c3}]$. The contributions from the individual sources $[I(s_1)\ I(s_2)\ I(s_3)]$ are modulated with a sinusoid that depends on the camera polarizer angle and the light source direction. That is,

$$\begin{bmatrix} I(\theta_{c1}) \\ I(\theta_{c2}) \\ I(\theta_{c3}) \end{bmatrix} = \begin{bmatrix} m_{11} & m_{12} & m_{13} \\ m_{21} & m_{22} & m_{23} \\ m_{31} & m_{32} & m_{33} \end{bmatrix} \begin{bmatrix} I(s_1) \\ I(s_2) \\ I(s_3) \end{bmatrix}. \quad (1)$$

The matrix $M = [m_{ij}]$, $i, j = 1 \ldots 3$, contains the modulation coefficients where each row corresponds to a fixed camera polarizer angle and each column corresponds to a fixed light source direction. Therefore, demultiplexing can be done to obtain the individual contributions $[I(s_1)\ I(s_2)\ I(s_3)]$ by inverting the matrix M.

2.1 Intensity Modulation

The modulation coefficients in (1) can be derived as follows: Let l be the illumination direction, p_s is the light source polarizer direction, p_c is the camera polarizer direction, and p is the polarization direction of the incident ray, as illustrated in Fig. 1.

- *O.G. Cula is with Johnson & Johnson, CPCW, 199 Grandview Road, Skillman, NJ 08558. E-mail: oanacula@caip.rutgers.edu.*
- *K.J. Dana is with the Department of Electrical and Computer Engineering, Rutgers University, 94 Brett Road, Piscataway, NJ 08854-8058. E-mail: kdana@ece.rutgers.edu.*
- *D.K. Pai is with the Department of Computer Science, 2366 Main Mall, University of British Columbia, Vancouver, B.C. V6T 1Z4, Canada. E-mail: pai@cs.ubc.ca.*
- *D. Wang is with the Department of Computer Science, Rutgers University, 110 Frelinhuysen Road, Piscataway, NJ 08854. E-mail: dswang@cs.rutgers.edu.*

Manuscript received 28 July 2005; revised 21 Jan. 2006; accepted 9 June 2006; published online 13 Dec. 2006.
Recommended for acceptance by G. Finlayson.
For information on obtaining reprints of this article, please send e-mail to: tpami@computer.org, and reference IEEECS Log Number TPAMI-0405-0705.

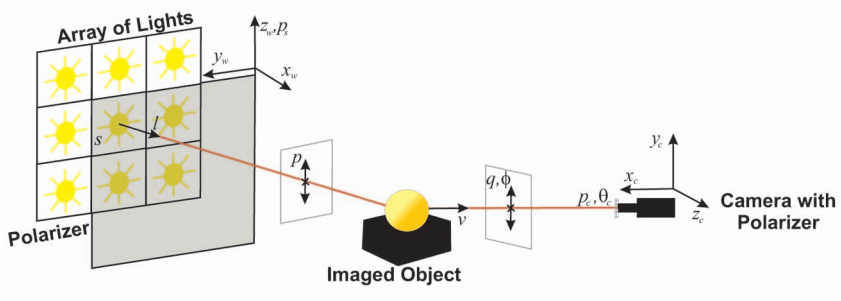

Fig. 1. An object is imaged with multiple light sources. A linear polarized sheet is placed in front of the light sources with polarization direction p_s. The z-axis z_w of the world coordinate frame W is aligned with p_s. The light source direction is denoted by l, while the viewing direction is v. The polarization direction in the plane perpendicular to the direction of the incident light is p. The polarization direction and the corresponding polarization angle of the reflected light (defined in the camera plane) are q and ϕ. A linear polarizer placed on the camera lens has polarization direction p_c and a corresponding polarizer angle of θ_c.

We consider only the surface (specular) reflectance component that retains the polarization of the source. Depending on the material in the scene, the body (diffuse) reflectance may not be completely depolarized and the degree of polarization may have an angular dependence, as the Fresnel reflectance model [26], [25] states. However, we approximate that the body component of the reflectance becomes depolarized, and this simplification works sufficiently for our purpose of separating the contributions from different sources to the surface reflectance.

The electric field vector of the light at the camera has a particular polarization direction in the imaging plane which we call q. Therefore, the electric field vector at the camera polarizer is $E = |E|q$. With no camera polarizer the intensity captured by the camera sensor would be $I = EE^* = |E|^2$. When the light ray passes the camera polarizer, the electric field vector becomes $E = (|E| \cos\theta)p_c$, where θ is the angle between the camera polarizer and the polarization of the light ray at the camera. The image intensity $I(\theta_c)$ with the camera polarizer rotated by θ_c is given by

$$I(\theta_c) = EE^* = |E|^2 \cos^2\theta_c. \tag{2}$$

This expression can be written to explicitly show the dependence on the camera polarizer angle θ_c and the light source s,

$$I(\theta_c, s) = (p_c \cdot q)^2 I(s), \tag{3}$$

where $I(s)$ is the intensity in the image due to source s without the camera polarizer.

We define a world coordinate frame W, where the z-axis is aligned with p_s so that ${}^W p_s = [0, 0, 1]$. To get p, the polarizer direction p_s gets projected onto the plane perpendicular to the incident ray vector. That is, subtract from p_s the component parallel to l (assume l is the illumination direction) to get

$$p = p_s - (p_s \cdot l)\, l. \tag{4}$$

In world coordinates,

$${}^W p = \left(\begin{bmatrix} 0 \\ 0 \\ 1 \end{bmatrix} - l_z \begin{bmatrix} l_x \\ l_y \\ l_z \end{bmatrix} \right) = \begin{bmatrix} -l_x l_z \\ -l_z l_y \\ 1 - l_z^2 \end{bmatrix} \frac{1}{\sqrt{1 - l_z^2}}. \tag{5}$$

This equation reveals that the polarization direction p depends on the illumination direction.

We arrange the camera so that the y-axis of the image plane is coincident with the z-axis of the world coordinate frame and, therefore, coincident with p_s, the polarizer direction at the source. The angle that p makes with z_w in the plane perpendicular to l is the same as the angle q makes with z_w in the plane perpendicular to v (i.e., the image plane). This angle is given by

$$\phi = \arccos(p \cdot z_w) = \arccos(\sqrt{1 - l_z^2}). \tag{6}$$

The angle ϕ depends on l_z which in turn depends on the source s. For multiple sources, the notation ϕ_j is used for $\phi(s_j)$. The intensity I due to source s_j is given by

$$I(\theta_c, s_j) = (p_c \cdot q)^2 I(s_j) = \cos^2(\theta_c - \phi_j) I(s_j). \tag{7}$$

Notice that the intensity is a function of θ_c and l_z. Therefore, the approach can separate sources that have different l_z values. If the illumination vectors have the same l_z value, the phases do not vary and the light sources cannot be demultiplexed. This situation occurs when the light sources are positioned in a plane perpendicular to p_s. Pseudoinverse and singular value decomposition techniques are employed to avoid numerical problems in the implementation due to this degeneracy.

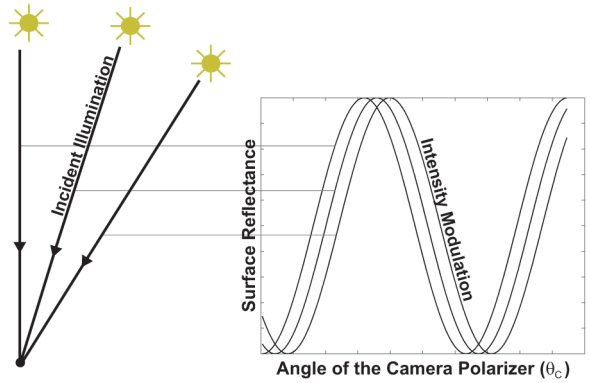

Fig. 2. Because the light is polarized, there is a sinusoidal modulation of the intensity as a function of the camera polarizer angle. In addition, different angles of the incident illumination have modulation functions with different phases.

2.2 Demultiplexing Algorithm

We consider the situation where multiple light sources illuminate the scene simultaneously as shown in Fig. 1. The aggregate intensity is given by

$$I(\theta_c) = \sum_{j=1}^{N} \cos^2(\theta_c - \phi_j) I(s_j), \tag{8}$$

or

$$I(\theta_c) = \frac{1}{2} \sum_{j=1}^{N} (1 + \cos 2\theta_c \cos 2\phi_j + \sin 2\theta_c \sin 2\phi_j) I(s_j), \tag{9}$$

where N is the number of sources, or

$$I(\theta_c) = MI(s). \tag{10}$$

Each camera polarization angle θ_c and each source direction gives a different attenuation curve. At a surface point, the incident light is the sum of individual light sources multiplied by a

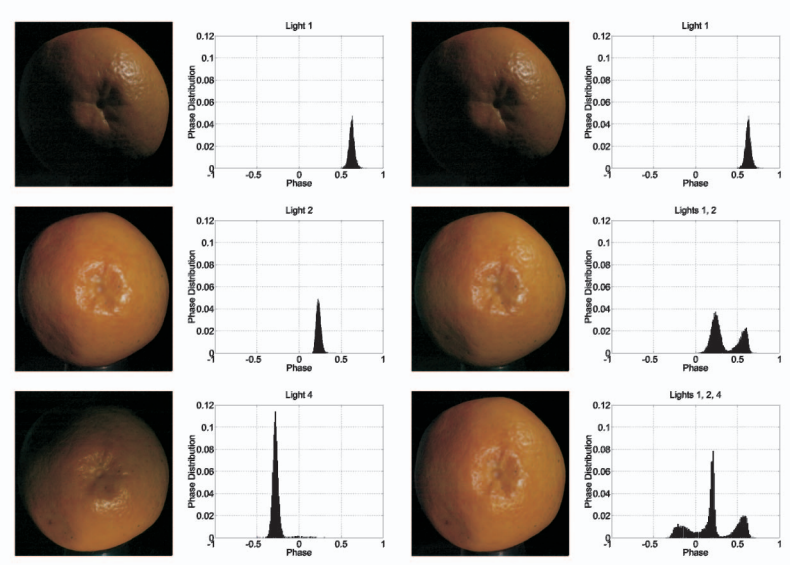

Fig. 3. First column: The orange is illuminated by one light source, for three different light sources. Second column: The corresponding phase histograms for the three cases in the first column. Notice how distinct light directions give rise to distinct cluster centers in the phase space (see (6)). Third column: The orange is imaged with three sources, added one at a time. Fourth column: The phase histograms corresponding to the three cases in the third column. Note that the number of clusters in the phase space equals the number of light sources illuminating the scene.

polarization attenuation coefficient that depends on the light source direction and the camera polarizer.

Note that since M can be factored into two matrices (as (9) suggests), we know that the rank of M cannot be greater than the rank of these factor matrices. That is

$$M = M_a M_b,$$
$$rank(M) \leq rank(M_a),$$
$$rank(M) \leq rank(M_b).$$

Therefore, the rank of M is at most 3. So, for each multiplexing stage, the individual contributions of three sources can be estimated. Demultiplexing is simply inverting (10) to obtain

$$I(s) = M^{-1} I(\theta_c). \tag{11}$$

We extend the result to an arbitrary number of sources in Section 3.2.

To construct matrix M of (10) the camera polarizer angle θ_c and the sinusoid phase ϕ_j must be known. The camera polarizer angle θ_c is calibrated with respect to the camera. Using images of the scene under multiple camera polarizer angles, we can get an estimate of the modulation sinusoid *at each pixel*. Note that few images are needed to fit this sinusoid; in fact, only two are required according to the Nyquist sampling theory. In practice, we use three images, i.e., three camera polarizer angles. Since the phase of the modulating function is estimated for each pixel, we can construct a phase histogram as shown in Fig. 6. We estimate the source phase ϕ_j as the center of the modes in the phase distribution, illustrated in Fig. 3. The light source positions need not be known.

Polarization demultiplexing necessitates a linear camera, and we use the methods in [3] to estimate the camera response, such that we could translate the image intensities into reflectance space, where superposition is valid.

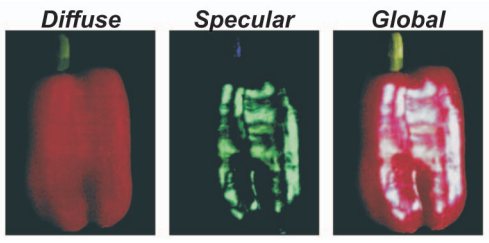

Fig. 4. The diffuse component, the specular component, and the superposition of the two components.

3 Results

For the experimental results, we imaged several objects with various material properties or geometries using a Nikon D2H single lens reflex digital camera, equipped with Nikon Nikkor 28-80mm f/3.3-5.6G autofocus lens. The lens is augmented with a rotating linear polarizer glass filter. The light setup consists of 24 LED bulbs,[1] arranged as a 6×4 array. Between the light array and the imaged scene, we position a linearly polarizing screen.[2]

3.1 Multiplexing with Three Sources

A pepper is simultaneously illuminated by three different light sources, and the scene is imaged with three directions for the linear polarizer at the camera: $\{0, 2\pi/5, 4\pi/5\}$. One of these input images is illustrated in the left image of Fig. 5. Note that the camera polarizer angle θ_c is calibrated with respect to the camera. The separated components, i.e., diffuse and specular, are illustrated in Fig. 4, along with the superposition of these two. The separation is done by using the estimated modulation function at each pixel where the body reflectance is the constant component. Note that in this image, obtained by adding the body and surface reflectance, all specularities are present, as if the polarizer at the camera is not present.

The phase distributions for the specular points in the scene, for each color channel (see Fig. 6), show three modes, i.e., three illumination sources are detected. Given the input images and applying our polarization demultiplexing technique, we obtain the demultiplexed specularities, as shown in Fig. 5. The demultiplexed specularities are shown superimposed over the body reflectance. The ground truth (the pepper illuminated with each light source individually) is also shown in Fig. 5. By comparing our results and the ground truth, observe that indeed the demultiplexed specularities are similar to those in the ground truth images, indicating

1. www.SuperBrightLeds.com.
2. Edmund Optics, Tech Spec Linear Polarizing Laminated Film.

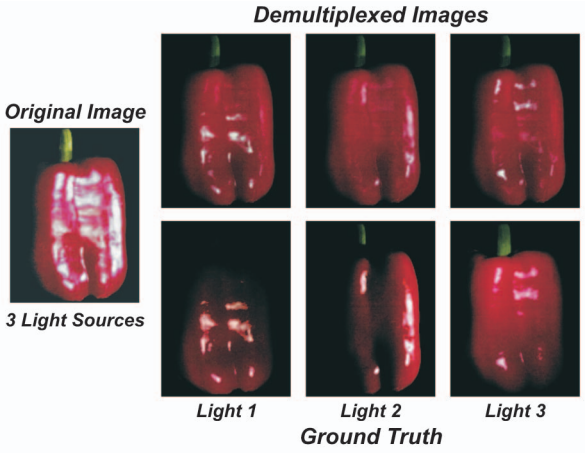

Fig. 5. Demultiplexing results for a pepper. The pepper is viewed with multiple light sources (left). Demultiplexed images that show the pepper as it would appear when illuminated by individual light sources separately (center and right, first row). Note that the surface reflection in the demultiplexed images matches the surface reflectance in the ground truth images (center and right, second row).

successful demultiplexing. The diffuse component differs for ground truth images and the demultiplexed images, as expected, because polarization multiplexing works for the surface (specular) reflectance. The diffuse component as a function of illumination direction can be readily modeled with existing methods [21].

3.2 Multiplexing with More Than Three Sources

When the scene is illuminated by $N > 3$ light sources, matrix M in (10) is still rank 3, therefore, M is not invertible. We modify the polarization multiplexing method by adding $N-3$ additional imaging sessions. During each additional imaging session, one of the lights illuminating the scene is not polarized and multiple images of the scene are acquired, as the polarizer at the camera is rotated. We use a linearly polarizing screen with a slit, such that by sliding the polarizing screen between the lighting environment and the scene, one light source remains unpolarized. The unpolarized light will give rise to surface reflectance which is not modulated by a sinusoid. We identify which light source is unpolarized by inspecting the phase distribution computed for each of the additional imaging sessions, i.e., by identifying the missing mode

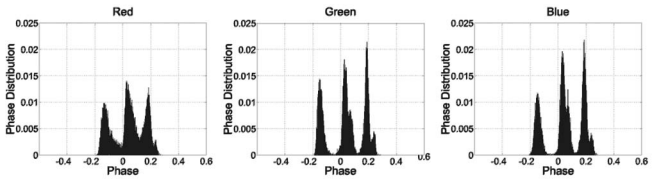

Fig. 6. The phase distribution for the specular points in the pepper scene illustrated in Fig. 5, for each color channel.

in the phase distribution. We construct M as follows: the first three rows are defined as in (8); the following $N-3$ rows are similarly defined, but they have a zero in the column corresponding to the unpolarized light source. Now, matrix M has rank N and it is invertible. By using (11), we demultiplex the surface reflectance due to each of the N sources illuminating the scene.

Fig. 7 exemplifies how polarization demultiplexing works for the case of five sources illuminating the scene. First, all sources are covered by the polarizing screen and the corresponding phase histogram shows five modes, each corresponding to a source illuminating the scene. Then, the polarizing screen is placed between the scene and the lighting environment such that one source is not polarized. Again, the scene is imaged with three polarizer angles at the camera. The corresponding phase distribution has four modes only, because the unpolarized source gives rise to unmodulated surface reflectance. From the phase distribution, it can be seen that light 4 is not polarized. And, finally, the scene is imaged again with the polarizer screen moved in a different position. The phase distribution has four modes, showing that light 2 is not polarized. Demultiplexing is performed using these three sets of data. Fig. 7 shows that the results are very similar with the ground truth images, acquired with just one source illuminating the scene.

It is interesting to analyze the conditions under which matrix M becomes singular and cannot be inverted. This could happen whenever a row or a column of M is a linear combination of other rows or columns, respectively. M becomes ill-conditioned whenever the camera polarizer angles θ_c are sampled within a very narrow interval, and not across the entire period of $[0, \pi]$. To avoid this degeneracy, we typically use camera polarizer angles θ_c that are sampled equally spaced across the interval $[0, \pi]$. Again, M

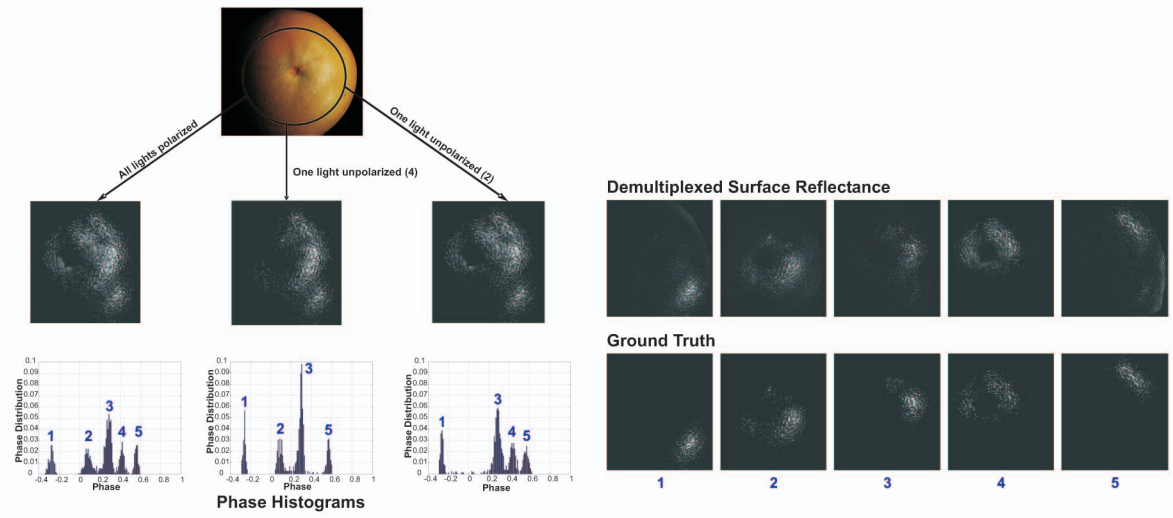

Fig. 7. Multiplexing with more than three sources. The orange is illuminated by five sources. First, all five lights are polarized. The phase distribution has five modes. Then, only four sources are polarized. The phase distribution has four modes, showing that light 4 is not polarized. And finally, the scene is imaged with four polarized lights, while light 2 is not polarized. Demultiplexing is performed with these three sets of data. The results are very similar with the ground truth images.

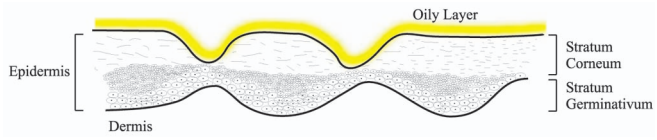

Fig. 8. Skin structure includes complex geometry and an oily layer at the air-skin interface, as well as layers of cells in the stratum corneum and stratum germinativum of the epidermis. Such layers give rise to reflection and interreflection at multiple interfaces.

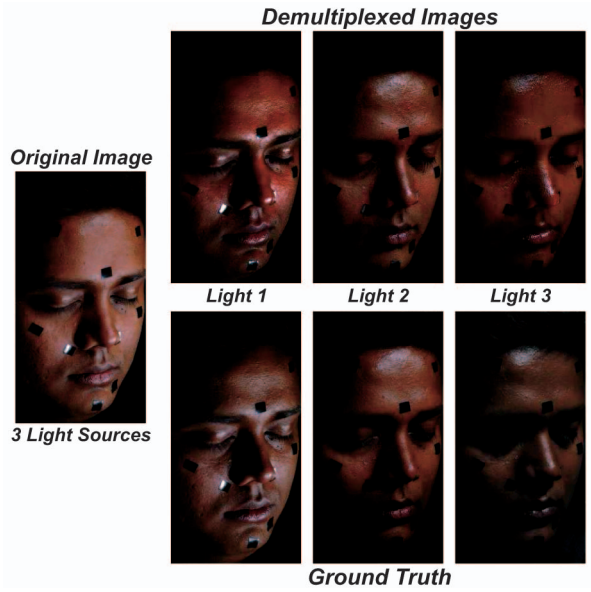

Fig. 9. Demultiplexing results for a human face. The face is viewed with multiple light sources (left). Demultiplexed images that show the face as it would appear when illuminated by individual light sources separately (center and right, first row). Note that the surface reflection in the demultiplexed images matches the surface reflectance in the ground truth images (center and right, second row).

could become ill-conditioned when the source phases ϕ are gathered together within a narrow interval. In this case, the pseudoinverse and singular value decomposition techniques are used to avoid numerical problems.

3.3 Polarization Multiplexing for Skin Modeling

A simplified skin reflectance model consists of the surface component due to the oily layer and the subsurface component due to scattering in the epidermis as shown in Fig. 8. For skin modeling, high quality models have been introduced for subsurface scattering, [9], [7], [6], [24]. However, the surface reflectance component is necessary to obtain realistic skin appearance. The surface reflectance component shows the fine-scale skin geometry including pores and wrinkles.

The typical approach for rendering this component is to use masks that create a cast of the face [7], [10]. These masks are scanned and the fine scale geometry is rendered on the face using a shading model. However, this approach has several disadvantages: 1) a point-wise shading model applied to the measured geometry is an oversimplification and does not represent real optical effects including interreflections at multiple interfaces, 2) the measured shape may not be entirely accurate due to mask material pressing on the skin, and 3) mask creation is a cumbersome approach to modeling. So, appearance-based modeling is particularly well suited for the surface reflectance component of skin.

Polarization demultiplexing is especially useful when imaging the surface reflectance of human faces. With multiple sources, the dynamic range of the camera is properly utilized and the signal to noise ratio is high. In Fig. 9, we show results for a scene comprised

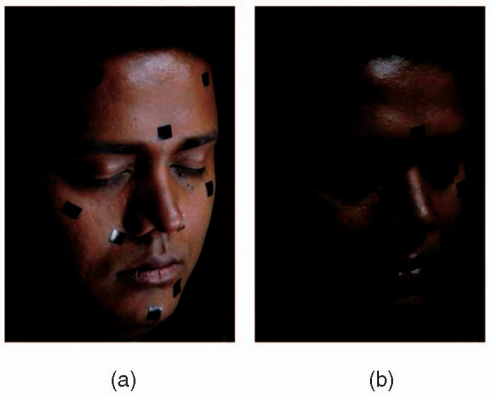

Fig. 10. Two examples of original face images. (a) The face is imaged with all three lights on, with an exposure time of 1/6 seconds. (b) The face is imaged with one light only, while the exposure time is set to 1/3 seconds. Observe the reduced the dynamic range of the image on the right, even though the exposure time is twice as much as that used for the left image.

of a human face illuminated simultaneously by three source clusters. A source cluster is composed of four smaller sources, grouped in a cluster. The light intensity from one cluster is not sufficient to capture face images with a good signal-to-noise ratio. When the scene is comprised of inanimate objects, such as an orange, the exposure time can be increased without restrictions. However, absolute stillness is not possible with a human subject. Breathing and involuntary movements cause unacceptable loss of detail. During our experiments, we observed that an exposure time larger than 1/3 seconds induces a blurred image. Fig. 10 shows that the dynamic range is quite reduced when the image is captured with one light cluster (Fig. 10b), as opposed to the dynamic range of the image captured with three light clusters (Fig. 10a). Note that Fig. 10b has been captured with an exposure time of 1/3 seconds, while Fig. 10a has been captured with an exposure time of 1/6 seconds.

In Fig. 9, on the left, the face is viewed with multiple light sources. On the right, on the first row, the demultiplexed images show the face as it would appear when illuminated by individual source clusters separately. The demultiplexed contributions to surface reflectance match the surface reflectance due to each source cluster, illustrated by the ground truth images (see Fig. 9, second row on the right).

3.4 Identifying the Number of Sources

We image a scene comprised of an orange, illuminated by only one light source at a time, for three different sources, as shown in the first column of Fig. 3. From the corresponding phase distributions, shown in the second column of Fig. 3, we can see that different light directions give rise to different locations of the clusters in phase space. Moreover, to test the separability of these modes in a more complex illumination configuration, the orange is imaged with three sources, added one at a time, as illustrated in the third column of Fig. 3. That is, the first image in the column has one light source, the second has two light sources, etc. The corresponding phase distributions, plotted in the fourth column of the same figure, clearly show that the number of clusters in the phase space equals the number of sources illuminating the scene; therefore, the phase carries information about the scene illumination.

4 Conclusion and Summary

In both computer vision and graphics, there is significant interest in layered models, which decompose the image into body and

surface reflectance, to determine how each varies with view and illumination. The body reflectance can often be well modeled with known parametric models using a small number of images. On the other hand, fine-scale surface geometry causes local shadows and occlusions so more image samples are needed to capture surface reflectance. Polarization multiplexing provides a convenient way to obtain images under multiple illumination directions and therefore has a significant impact on appearance-based modeling. Rather than imaging the scene with one light source at a time, the imaging process is significantly simplified by illuminating the scene with multiple sources. Then, polarization demultiplexing can be employed to isolate the contributions of individual sources to surface reflectance. Moreover, illuminating the scene with multiple sources allows a reduced exposure time at a good signal to noise ratio (especially important when imaging human subjects).

Furthermore, a scene might be simultaneously illuminated by a complex configuration of light sources that cannot be controlled, e.g., ordinary overhead lighting that only has one switch for all lights. In order to learn how each light source affects the appearance, our polarization-based measurement protocol can be used. In fact, the approach can be used any time a polarizing screen can be placed between the scene and the lighting. The resulting measurements provide information about the number of sources illuminating the scene. Moreover, by using polarization multiplexing, one can separate the effect of each source on surface reflectance.

ACKNOWLEDGMENTS

This material was based upon work supported by the US National Science Foundation under Grant No. 0092491, Grant No. 0085864, Grant IIS-0308157, and Grant EIA-0215887.

REFERENCES

[1] O.G. Cula, K.J. Dana, F. Murphy, and B.K. Rao, "Skin Texture Modeling," *Int'l J. Computer Vision,* vol. 62, nos. 1-2, pp. 97-119, Apr.-May 2005.
[2] K.J. Dana, B. van Ginneken, S.K. Nayar, and J.J. Koenderink, "Reflectance and Texture of Real World Surfaces," *ACM Trans. Graphics,* vol. 18, no. 1, pp. 1-34, Jan. 1999.
[3] P.E. Debevec and J. Malik, "Recovering High Dynamic Range Radiance Maps from Photographs," *Proc. ACM SIGGRAPH,* pp. 369-378, Aug. 1997.
[4] P.E. Debevec, T. Hawkins, C. Tchou, H.-P. Duiker, W. Sarokin, and M. Sagar, "Acquiring the Reflectance Field of a Human Face," *Proc. ACM SIGGRAPH,* pp. 145-156, 2000.
[5] C. Donner and H.W. Jensen, "Light Diffusion in Multi-Layered Translucent Materials," *Proc. ACM SIGGRAPH,* pp. 1208-1215, Aug. 2005.
[6] P. Hanrahan and W. Krueger, "Reflection from Layered Surfaces Due to Subsurface Scattering," *Proc. ACM SIGGRAPH,* pp. 165-174, 1993.
[7] A. Haro, B. Guenter, and I. Essa, "Real-Time, Photo-Realistic, Physically Based Rendering of Fine Scale Human Skin Structure," *Proc. 12th Eurographics Workshop Rendering,* pp. 53-62, June 2001.
[8] T. Hawkins, A. Wegner, C. Tchou, A. Gardner, F. Goransson, and P. Debevec, "Animatable Facial Reflectance Fields," *Proc. Eurographics Symp. Rendering,* pp. 309-321, 2004.
[9] H.W. Jensen, S.R. Marschner, M. Levoy, and P. Hanrahan, "A Practical Model for Subsurface Light Transport," *Proc. ACM SIGGRAPH,* pp. 511-518, 2001.
[10] H.W. Jensen, "Digital Face Cloning," *Proc. ACM SIGGRAPH,* July 2003.
[11] M.L. Koudelka, S. Magda, P.N. Belhumeur, and D.J. Kriegman, "Acquisition, Compression and Synthesis of Bidirectional Texture Functions," *Proc. Third Int'l Workshop Texture Analysis and Synthesis,* pp. 59-64, Oct. 2003.
[12] H.P.A. Lensch, J. Kautz, and M. Goesele, W. Heidrich, and H.P. Seidel, "Image-Based Reconstruction of Spatial Appearance and Geometric Detail," *ACM Trans. Graphics,* vol. 22, no. 2, pp. 234-257, Apr. 2003.
[13] D. Miyazaki, M. Saito, Y. Sato, and K. Ikeuchi, "Determining Surface Orientations of Transparent Objects Based on Polarization Degrees in Visible and Infrared Wavelengths," *J. Optical Soc. Am.,* vol. 19, no. 4, pp. 687-694, Apr. 2002.
[14] D. Miyazaki, R.T. Tan, K. Hara, and K. Ikeuchi, "Polarization-Based Inverse Rendering in a Single View," *Proc. Int'l Conf. Computer Vision,* pp. 982-987, 1997.
[15] S.K. Nayar, X.S. Fang, and T. Boult, "Separation of Reflection Components Using Color and Polarization," *Int'l J. Computer Vision,* vol. 21, no. 3, pp. 163-186, Feb. 1997.
[16] C.S. Ng and L. Li, "A Multi-Layered Reflection Model of Natural Human Skin," *Computer Graphics Int'l,* pp. 249-256, 2001.
[17] K. Nishino, Y. Sato, and K. Ikeuchi, "EigenTexture Method: Appearance Compression and Synthesis Based on a 3D Model," *IEEE Trans. Pattern Analysis and Machine Intelligence,* vol. 23, no. 11, pp. 1257-1265, Nov. 2001.
[18] S. Rahmann and N. Canterakis, "Reconstruction of Specular Surfaces Using Polarization Imaging," *Proc. IEEE Conf. Computer Vision and Pattern Recognition,* pp. 149-155, 2001.
[19] M. Saito, Y. Sato, K. Ikeuchi, and H. Kashiwagi, "Measurement of Surface Orientations of Transparent Objects Using Polarization in Highlight," *Proc. IEEE Conf. Computer Vision and Pattern Recognition,* vol. 1, pp. 381-386, 1999.
[20] Y.Y. Schechner, J. Shamir, and N. Kiryati, "Polarization-Based Decorrelation of Transparent Layers: The Inclination Angle of an Invisible Surface," *Proc. Int'l Conf. Computer Vision,* pp. 814-819, 1999.
[21] Y.Y. Schechner, S.K. Nayar, and P.N. Belhumeur, "A Theory of Multiplexed Illumination," *Proc. Int'l Conf. Computer Vision,* pp. 808-815, 2003.
[22] N. Tsumura, N. Ojima, K. Sato, M. Shiraishi, H. Shimizu, H. Nabeshima, S. Akazaki, K. Hori, and Y. Miyake, "Image-Based Skin Color and Texture Analysis/Synthesis by Extracting Hemoglobin and Melanin Information in the Skin," *ACM Trans. Graphics,* vol. 22, no. 3, pp. 770-779, July 2003.
[23] M.A.O. Vasilescu and D. Terzopoulos, "TensorTextures," *Proc. ACM SIGGRAPH,* pp. 336-342, 2004.
[24] L. Williams, "The Gemini Man," *Proc. ACM SIGGRAPH,* Digital Face Cloning: Course in Siggraph, 2005.
[25] L.B. Wolff and T.E. Boult, "Constraining Object Features Using a Polarization Reflectance Model," *IEEE Trans. Pattern Analysis and Machine Intelligence,* vol. 13, no. 7, pp. 635-657, July 1991.
[26] L.B. Wolff, "Polarization-Based Material Classification from Specular Reflection," *IEEE Trans. Pattern Analysis and Machine Intelligence,* vol. 12, no. 11, pp. 1059-1071, Nov. 1990.